

Title Page

A dioxin-responsive enhancer 3' of the human *CYP1A2* gene

Steven T. Okino, Linda C. Quattrochi, Deepa Pookot, Mieko Iwahashi and Rajvir Dahiya

Department of Urology, San Francisco Veterans Affairs Medical Center and the University of California
San Francisco, San Francisco, CA 94121 (STO, DP and RD)

Department of Medicine, School of Medicine, University of Colorado at Denver and Health Sciences
Center, Denver, CO 80262 (LCQ and MI)

Running Title Page

Running Title: A TCDD-responsive *CYP1A2* enhancer

Corresponding author:

Rajvir Dahiya

Department of Urology

San Francisco Veterans Affairs Medical Center and UCSF

4150 Clement Street

Building 203 room 2B-24 (112F)

San Francisco, CA 94121

Tel: (415) 221-4810 x6964

Fax: (415) 750-6639

E-mail: Rdahiya@urology.ucsf.edu

Number of text pages: 29

Number of tables: 1

Number of figures: 6

Number of references: 40

Number of words in abstract: 250

Number of words in introduction: 430

Number of words in discussion: 870

Abbreviations: AhR, aryl hydrocarbon receptor; TCDD, 2,3,7,8-tetrachlorodibenzo-*p*-dioxin; PAH, polycyclic aromatic hydrocarbon; DRE, dioxin-response element; GAPDH, glyceraldehyde-3-phosphate dehydrogenase; ChIP, chromatin immunoprecipitation; DMS, dimethyl sulfate.

Abstract

The human *CYP1A* genes, *CYP1A1* and *CYP1A2*, are in a head-to-head orientation on chromosome 15. Both *CYP1A* genes, as well as *CYP1B1*, are transcriptionally induced by the aryl hydrocarbon receptor (AhR), a ligand-activated transcription factor that binds 2,3,7,8-tetrachlorodibenzo-*p*-dioxin (TCDD, dioxin). Although the TCDD-responsive enhancers for *CYP1A1* and *CYP1B1* are well characterized, a similar *CYP1A2* enhancer has not been identified. In the human prostate cell line RWPE-1, *CYP1A2* mRNA expression is dramatically induced by TCDD. Therefore, analysis of the native *CYP1A2* gene in these cells can provide insight into its induction mechanism. To identify sites that may bind AhR on the *CYP1A* locus we scanned 75 kb of chromosome 15 sequence for high affinity AhR binding sites. We then analyzed most of the sites for TCDD-inducible AhR interaction by chromatin immunoprecipitation. As expected, the *CYP1A1* and *CYP1B1* enhancers bind AhR in TCDD-treated cells. Importantly, we identify a region 3' of *CYP1A2* that binds AhR in response to TCDD. We cannot detect AhR binding at other sites on the *CYP1A* locus. *In vivo* footprinting demonstrates that two AhR binding sites in *CYP1A2*'s 3' region are occupied in TCDD-treated cells. Reporter-gene studies show that these sites confer TCDD-responsiveness to a heterologous promoter. AhR also binds to *CYP1A2*'s 3' region in TCDD-treated LS180 cells, but not in HepG2 and ND-1 cells. In the latter cell lines *CYP1A2*'s 3' region is extensively methylated. In summary, we identify a novel TCDD-responsive enhancer for *CYP1A2*. Surprisingly, this enhancer is not conserved across species and is primarily human-specific.

Introduction

The *CYP1* gene family, *CYP1A1*, *CYP1A2*, and *CYP1B1*, encode cytochrome P-450s that metabolize a wide variety of structurally diverse chemicals and are implicated in both their detoxification and bioactivation into carcinogenic and toxic compounds. All members of the *CYP1* gene family are transcriptionally induced by the aryl hydrocarbon receptor (AhR), a ligand-activated transcription factor that binds polycyclic aromatic hydrocarbons (PAHs) and halogenated aromatic hydrocarbons with high affinity. 2,3,7,8-tetrachlorodibenzo-p-dioxin (TCDD, dioxin), a notorious environmental contaminant, has the highest affinity for AhR and is the most potent inducer of the *CYP1* genes (Poland and Knutson, 1982; Schmidt and Bradfield, 1996; Whitlock et al., 1997; Nebert et al., 2004; Shimada and Fujii-Kuriyama, 2004; Nebert and Dalton, 2006).

The most well studied dioxin-response is the transcriptional induction of *CYP1A1*. TCDD induces *CYP1A1* by binding to and activating AhR which then translocates to the nucleus and interacts with its partner protein ARNT to form an active heteromeric transcription factor. The AhR complex then interacts with DNA binding sites, termed dioxin-response elements (DREs), located on the *CYP1A1* enhancer to mediate TCDD-inducible gene expression (Hankinson, 1995; Whitlock, 1999). Like *CYP1A1*, the TCDD-responsive *CYP1B1* enhancer contains DRE sites upstream of its transcriptional start site that bind AhR and mediate TCDD-inducible gene expression (Zhang et al., 1998; Tsuchiya et al., 2003).

Unlike the other *CYP1* genes, the mechanism by which TCDD-induces *CYP1A2* is not well understood. A non-consensus DRE that binds AhR *in-vitro* and confers TCDD-responsiveness to a reporter gene has been identified upstream of the *CYP1A2* promoter (Quattrochi and Tukey, 1989; Postlind et al., 1993; Quattrochi et al., 1994). However, the *in-vivo* functionality of this site has not been established. Also, because the *CYP1A1* and *CYP1A2* genes are positioned in a head-to-head orientation they share a common 5' upstream region. Thus, the *CYP1A1* enhancer might also control *CYP1A2* expression (Corchero et al., 2001). Indeed, a reporter gene study demonstrates that the *CYP1A1* enhancer confers TCDD-inducibility on the distant *CYP1A2* promoter (Ueda et al., 2006). In addition, transgenic

mice containing 85 kb of human DNA containing both *CYP1A* genes induce *CYP1A2* in response to TCDD. In contrast, a 50 kb transgene containing *CYP1A2*, but lacking the *CYP1A1* enhancer region did not (Jiang et al., 2005). Together, these findings imply that the TCDD-responsive *CYP1A1* enhancer also controls *CYP1A2* expression. However, a significant caveat of these studies is that *CYP1A2* was analyzed outside of its native setting, either as a reporter plasmid or as a transgene. Here we analyze the endogenous *CYP1A2* gene in several human cell lines. We identify a novel TCDD-responsive, AhR-dependent enhancer 3' of the human *CYP1A2* gene.

Materials and Methods

Cells and cell culture. RWPE-1, HepG2 and LS-180 cells were obtained from the American Type Culture Collection (Manassas, VA) and cultured as directed. RWPE-1 cells are normal human adult epithelial prostate cells that have been immortalized by transfection with a plasmid containing the human papilloma virus. HepG2 cells are a human hepatocellular carcinoma cell line. LS-180 cells are a human colonic adenocarcinoma cell line. ND-1 cells, a human primary prostatic adenocarcinoma cell line, was developed in our laboratory and cultured as described (Narayan and Dahiya, 1992). Cells were treated with TCDD (10 nM, Wellington Laboratories Inc., Ontario, Canada) for 30 minutes to 18 hours.

Quantitation of mRNAs. Total RNA was isolated from 90% confluent plates of cultured cells using the RNeasy mini kit (Qiagen, Valencia, CA) according to the manufacturer's directions. Human liver and prostate total RNA was purchased from Clontech (Mountain View, CA). The liver RNA sample was from a 51 year old male Caucasian. The prostate RNA sample was from a pool of 32 male Caucasians ages 21-50. RT-PCR was performed using the Titanium One-Step RT-PCR Kit (BD Biosciences, San Jose, CA), following the manufacturer's directions. For conventional PCR CYP1A1 mRNA was amplified using the primers CYP1A1-F (5'-ATCCCAGGCTCCAAGAGTCCACCCT-3') and CYP1A1-R (5'-GCGGGTCTTTCCCAGGGTCAGCAT-3') using 30 cycles of 30s at 94°C, 30s at 63°C, and 1 min at 72°C. CYP1A2 mRNA was amplified using the primers CYP1A2-F (5'-CCACACCAGCCATTACAACCCTGCC-3') and CYP1A2-R (5'-TGCGCTGGCTCATCCTTGACAGTGC-3') using 35 cycles of 30s at 94°C, 30s at 63°C, and 1 min at 72°C. CYP1B1 mRNA was amplified using the primers CYP1B1-F (5'-CTGGCACTGACGACGCCAAGAGACT-3') and CYP1B1-R (5'-TGGTCTGCTGGATGGACAGCGGGTT-3') using 30 cycles of 30s at 94°C, 30s at 63°C, and 1 min at 72°C. AhR mRNA was amplified using the primers AhR-F (5'-CCACAGCAACAGCTGTGTCAGAAGATG-3') and AhR-R (5'-

CGGATGATGAAGTGGCTGAAGATGTGT-3') using 30 cycles of 30s at 94°C, 30s at 63°C, and 1 min at 72°C. Arnt mRNA was amplified using the primers Arnt-F (5'-GCTGGGAGATCAGAGCAAC GCTACAA-3') and Arnt-R (5'-TGTTTCTTTCCAGAGGGACTGCTCACA-3') using 30 cycles of 30s at 94°C, 30s at 63°C, and 1 min at 72°C. Glyceraldehyde-3-phosphate dehydrogenase (GAPDH) mRNA was amplified using the primers GAPDH-F (5'-TTGGTCGTATTGGGCGCCTGGTCAC-3') and GAPDH-R (5'-AGACGCCAGTGGACTGGCCGACGTA-3') using 28 cycles of 30s at 94°C, 30s at 63°C, and 1 min at 72°C. The amplified DNA was electrophoresed on a 2.5% agarose gel and visualized by staining with ethidium bromide.

Quantitative PCR was performed using CYP1A1, CYP1A2 and GAPDH TaqMan primers on a 7500 Fast Real-Time System as directed by the manufacturer (Applied Biosystems, Foster City, CA). In most cases two independent samples were analyzed. For the prostate and liver RNA samples one sample was analyzed. Each sample was analyzed in quadruplicate. GAPDH served as an internal control to normalize CYP1A mRNA expression data.

Chromatin immunoprecipitation (ChIP). ChIP analysis was performed using the protocol recommended for use with the EZ-ChIP kit (Upstate Biotechnology, Charlottesville, VA) with the following modifications: the cellular extract in ChIP dilution buffer was pre-cleared with protein A agarose/salmon sperm DNA (Upstate Biotechnology, Charlottesville, VA; 60 µl per ml extract) for 18 hours and then again for one hour at 4°C. The cleared cellular extract was then incubated with antibody (10 µl per ml extract) for one hour at 4°C. The antibody was then precipitated with protein A agarose/salmon sperm DNA (60 µl per ml extract) for 1 hour at 4°C. The protein A agarose-antibody/chromatin complex was then transferred to a small spin column (Qiagen, Valencia, CA) for washing. Three 400 µl washes were performed with each of the following buffers at room temperature; low salt immune complex wash buffer, high salt immune complex wash buffer, LiCl immune complex wash buffer, high salt LiCl immune complex wash buffer (1 M LiCl, 1% IGEPAL-CA630, 1% deoxycholic acid, 1 mM EDTA and 1 mM Tris, pH 8.1) and TE buffer. Following the last TE wash, the

small spin columns were transferred to a fresh collection tube and the protein-DNA complexes were eluted as indicated in the EZ-ChIP protocol. Following the cross-link reversal and RNase A/proteinase K digestion steps, the DNA was purified using the QIAquick PCR purification kit (Qiagen, Valencia, CA) as indicated by the manufacturer. The immunoprecipitated DNA was eluted in a total volume of 200 μ l. 10 μ l of DNA was analyzed in a 20 μ l PCR reaction using the following conditions: 3 minutes at 94°C, 30 cycles of 30 seconds at 94°C, 30 seconds at 60°C, and 30 seconds at 72°C followed by a 5 min 72°C extension step. The amplified DNA was electrophoresed on a 2.5% agarose gel and visualized by staining with ethidium bromide. The AhR antibody used in the immunoprecipitation was from Santa Cruz Biotechnology (H-211X; Santa Cruz, CA). The acetyl histone H4 antibody was purchased from Upstate Biotechnology. The sequences of the primers used in the ChIP analysis are as follows:

+15kb F (5'-AAATACAAAAATTAGCCAGGCATGG-3') and
+15kb R (5'-TGAAGTCTGTTCATATTCTTTGTCC-3');
+8kb F (5'-GAGACGGAGTTTCGATCTTTGTTGT-3') and
+8kb R (5'-CCGAGATCACCTGAGGACAGGAGTT-3');
+6kb F (5'-CAGCACAGTGATTAGGAGTCTTGTC-3') and
+6kb R (5'-TCCACCTCCTGGGCTCACACGATTC-3');
0kb F (5'-CCGCCACCTTTCTCTCCAATCCCAG-3') and
0kb R (5'-ATAGGCGGGCTTGTACGTGTGGCCA-3');
-0.5kb F (5'-TCAGGGCTGGGGTCGCAGCGCTTCT-3') and
-0.5kb R (5'-GCTACAGCCTACCAGGACTCGGCAG-3');
-1kb F (5'-TGACCTCTGCCCCCTAGAGGGATGT-3') and
-1kb R (5'-TTGGCAGAGCACAGAAATCCGGCGG-3');
-2kb F (5'-GATACTGGGGCGGTGAGGGGGGTTT-3') and
-2kb R (5'-TTATTCCCTCTGCCAGTTGCAGTCT-3');
-6k F (5'-CCCTGCTCCTGGTATTGATCACTAG-3') and
-6k R (5'-ACCTTGGCCTGGAGCTGAACACTCA-3');

-12kb F (5'-ACAGAATATTAGCCGGGCATGGTGG-3') and
 -12kb R (5'-GCTGCAAATGACAGGATCTCATTGG-3');
 -15kb F (5'-CATGATGGTGCCACTATACGCCAGC-3') and
 -15kb R (5'-CCTACTCTGGTCAGAGCCTCCTTCC-3');
 -19kb F (5'-AGCCTGTAATCTCAGCTACTCAGGA-3') and
 -19kb R: ATGAGCCCTGCTGTCAGGAGCATCT-3');
 -23k F (5'-ACTCAGTCTAGGCCAACCAGGCTCA-3') and
 -23k R (5'-CTTGGGCTGAAAATCAGGAGTGGCT-3');
 -33kb F (5'-GCTTGAACACCGGAGGCAGAGTTTG-3') and
 -33kb R (5'-GCAAAGTATGGCAATGCCTGCTTGC-3');
 -39kb F (5'-GCGCTCTGGGTCAGTGCCTCCACCA-3') and
 -39kb R (5'-AACGCGGTGAAACCCCATCTCTACT-3');
 -37kb F (5'-TTGAGCAGCATGGGGGTCTCCAGAC-3') and
 -37kb R (5'-TGGTAGCGTGCCAGGGAACAATGGG-3');
 -38kb F (5'-GATTCTCACGGCAAGAAGGACTCTC-3') and
 -38kb R (5'-CCAGCCAGGTATGTGCGTGTTTGTA-3');
 -44kb F (5'-TGAGGCAGGAGAATCGCTTGAACCC-3') and
 -44kb R (5'-AGTTGAACTCCTGGCAGGGAGTTAG-3');
 -47kb F (5'-ATCCTCACTCATCAGCAAAGCGGG-3') and
 -47kb R (5'-CCAAGTGACCAGCCAGCAGTGTGTT-3');
CYP1B1 enhancer F (5'-GGCAGCGCCCAGGGATATGACTGGA-3') and
CYP1B1 enhancer R (5'-CGGAGAGTGGCAGGAGGAGGCGAAT-3');
CYP1B1 promoter F (5'-TCCCATGAAAGCCTGCTGGTAGAGC-3') and
CYP1B1 promoter R (5'-CCACTCCAGAGTCAAAGCGCGCCAT-3');
GAPDH promoter F (5'-TACTAGCGGTTTTACGGGCGCACGT-3') and
GAPDH promoter R (5'-TCGAACAGGAGGAGCAGAGAGCGAA-3').

***In vivo* footprinting.** *In vivo* footprinting using dimethyl sulfate (DMS; Sigma, St. Louis, MO) was performed as described previously (Okino and Whitlock, 1995). To analyze the *CYP1A2*'s 3' enhancer we used the following primer set: Primer 1 (5'-ATGGGCAGATGTGGCCTGGA-3'); Primer 2 (5'-CTGGAGTGGTCAGGTGGATGCCTGT-3') and Primer 3 (5'-GTGGTCAGGTGGATGCCTGTGCGTGAG-3'). For primers 1, 2 and 3 the annealing temperatures were 50°C, 65°C; and 70°C respectively.

Construction of reporter genes. The pGL3-38k-wt reporter vector was constructed by cloning 112 bp of human chromosome 15 DNA sequence (see Fig. 3a) into the Nhe-I site of the pGL3-promoter vector (Promega, Madison, WI). pGL3-38k-mut, was identical to pGL3-38k-wt except that the sequence of the DRE sites were changed to prevent AhR binding (Fig 3a).

Transient transfections and luciferase activity assays. RWPE-1 and HepG2 cells were plated at a density of approximately 1.5×10^5 and 1.3×10^5 cells/well, respectively, in 24-well plates. Transfections were performed the following day using Fugene6 transfection reagent following the manufacturer's protocol (Roche Applied Science, Indianapolis, IN). The pDRE12 plasmid, a gift from Dr. Judy Raucy (Puracyp Inc., Carlsbad, CA), contains three copies of the consensus DRE subcloned into the pGL3-promoter vector and was used as a positive control for TCDD-inducible reporter gene activity (Yueh et al., 2005). For each transfection assay, 100 ng of luciferase reporter and 10 ng of pRL-SV40 (for transfection normalization; Promega, Madison, WI) were transfected into each well. The culture media was removed after incubation for 24 h with the transfection reagent-DNA complexes, and the cells were then treated for 24 h with 10 nM TCDD dissolved in DMSO. Control cells received media containing 0.1% DMSO. Following treatment, cells were rinsed with phosphate buffered saline (PBS) and luciferase assays were performed using the Dual-Luciferase Reporter Assay System (Promega, Madison, WI). Luciferase activity of cellular lysates was quantified with a Packard LumiCount luminometer. *Firefly*

luciferase activity was determined from three independent transfections, and normalized against *Renilla* luciferase activities of the pRL-SV40 vector obtained from the same culture.

Statistics. Statistics were performed using InStat Instant Statistics (Prism 4 GraphPad Software, San Diego, CA). Statistical differences between values were determined by two-tailed *t* test for comparing means from two groups. A *p* < 0.05 is considered statistically significant.

Bisulfite DNA sequencing. Genomic DNA was isolated from cultured cells using the AllPrep DNA/RNA Mini Kit (Qiagen, Valencia, CA) following the manufacturer's directions. Bisulfite modification of genomic DNA was performed using the EpiTect Bisulfite Kit (Qiagen, Valencia, CA) following the manufacturer's directions. Bisulfite-modified DNA was amplified using two rounds of PCR using nested primers that recognize the bisulfite modified DNA region 3' of *CYP1A2*. All primer sequences lack CpG sites and thus amplify methylated and unmethylated DNA equivalently. Sequences of the primers are as follows:

CYP1A2-3'-1f (5'-CTAACCCTACCCTAAACCTTACTAA-3');

CYP1A2-3'-2f (5'-ACCTTACTAACCTAAAATAACCCAA-3');

CYP1A2-3'-4r (5'-GGAAATGAGGGAAAAGGAGATAGAG-3').

PCR conditions were: 3 minutes at 94°C, 40 cycles of 30 seconds at 94°C, 30 seconds at 50°C, and 30 seconds at 72°C followed by a 5 min 72°C extension step. First round PCR was with the *CYP1A2*-3'-1f and *CYP1A2*-3'-4r primers. Second round PCR was performed using 1 µl of the first round PCR product in a total volume of 50 µl with the *CYP1A2*-3'-2f and *CYP1A2*-3'-4r primers. The amplification product was confirmed by electrophoresis on a 2% agarose gel and sequenced directly with the *CYP1A2*-3'-2f primer by an outside vendor (McLab, South San Francisco, CA).

Cross-species comparison of DNA homology. The cross-species comparison of DNA homology was performed using the vertebrate multiz alignment and conservation track on the UCSC genome browser (<http://genome.ucsc.edu/>) using the March 2006 human genome assembly (Kent et al., 2002).

Results

A cell culture model system to study TCDD-induction of *CYP1A2*. The dioxin-responsive enhancers of *CYP1A1* and *CYP1B1* are well characterized; they are both located 5' of the promoter and contain multiple DRE sites that bind AhR and confer TCDD-inducibility on a reporter gene (Hankinson, 1995; Zhang et al., 1998; Whitlock, 1999; Tsuchiya et al., 2003). In contrast, the location of *CYP1A2*'s enhancer is not clear due, at least in part, to the lack of a cell culture model system that expresses *CYP1A2* well. To identify a model system to analyze *CYP1A2* regulation we screened several human prostate cell lines for their ability to respond to dioxin. We find that in RWPE-1 cells, a normal human prostate epithelial cell line, the level of *CYP1A2* mRNA is dramatically increased by TCDD exposure; *CYP1A1* and *CYP1B1* are also strongly induced. In addition, the main components of the TCDD-response system, AhR and Arnt, are expressed constitutively (Fig 1). From these results we infer that analysis of the native *CYP1A2* gene in RWPE-1 cells can provide mechanistic insight into its induction by TCDD.

TCDD-inducible Ah Receptor binding 3' of *CYP1A2*. To identify sites that might bind AhR on the *CYP1A* locus we scanned 75 kb of human chromosome 15 DNA sequence for the high affinity DRE site: 5'-TNGCGTG-3' (Swanson et al., 1995). We find that in addition to the well characterized DRE sites on the *CYP1A1* enhancer, many other DRE sites exist (Fig 2a). We then analyzed most of these sites for the ability to interact with AhR by chromatin immunoprecipitation (Fig 2b). Some DNA regions have high sequence similarity with other genomic regions and were thus refractory to PCR analysis. As expected, the *CYP1A1* and *CYP1B1* enhancers exhibit strong TCDD-inducible interaction with AhR. Surprisingly, we also find that a region 3' of the *CYP1A2* gene (about -38 kb relative to the *CYP1A1* transcription start site) exhibits TCDD-inducible AhR binding. We cannot detect AhR binding at other sites on the *CYP1A* locus. A time-course experiment reveals that *CYP1A2*'s 3' region binds AhR with the same kinetics as the *CYP1A1* and *CYP1B1* enhancers indicating that binding there, like on *CYP1A1* and *CYP1B1*, is a primary response to TCDD (Fig 2c). These findings indicate that only two regions within the *CYP1A* locus have

the requisite *in-vivo* AhR-binding property expected of a dioxin-inducible AhR-dependent enhancer, the previously characterized *CYP1A1* enhancer and a novel region 3' of *CYP1A2*.

TCDD-inducible protein binding at DREs 3' of *CYP1A2*. Two high affinity DRE sites are contained within the AhR-binding *CYP1A2* region. These sites are separated by 87 bp and are in opposite orientations (Fig. 3a). We conducted an *in vivo* footprinting experiment to verify that these sites are indeed occupied by protein in response to dioxin (Fig. 3b). We treated control and TCDD-induced RWPE-1 cells with DMS, a reagent that modifies DNA in living cells. We then isolated genomic DNA and assessed the pattern and extent of DMS modification by ligation-mediated PCR. We observe a TCDD-inducible change in the DMS modification pattern at both of the DRE sites in *CYP1A2*'s 3' region. Within each DRE one base exhibits hyposensitivity and another base exhibits hypersensitivity to DMS modification. This TCDD-inducible change in the pattern of DRE modification is consistent with changes previously identified analyzing *CYP1A1* enhancer DREs in mouse and human cells (Wu and Whitlock, 1993; Kress et al., 1998; Okino et al., 2006). This implies that DRE sites 3' of *CYP1A2* are occupied in response to TCDD-exposure. This finding, together with our data analyzing AhR-DNA interaction (Fig. 2b), strongly suggests that AhR binds to two DRE sites located 3' of the endogenous *CYP1A2* gene.

***CYP1A2*'s 3' region is a TCDD-responsive enhancer.** We next performed a reporter-gene analysis to determine if *CYP1A2*'s 3' region can function as a TCDD-responsive enhancer. We constructed two reporter vectors using the pGL3 promoter backbone, one vector, termed pGL3-38k-wt, contains 112 bp of genomic DNA sequence including both DRE sites. The other vector, termed pGL3-38k-mut, was identical to the first except that the sequence of both DRE sites were changed to prevent AhR binding (Fig 3a). We then assayed the TCDD-responsiveness of these vectors as well as pDRE12, a TCDD-responsive control plasmid (Yueh et al., 2005), by transient transfection into RWPE-1 cells and HepG2 cells. Our results (Fig. 4) reveal that the pGL3-38k-wt reporter construct is inducible by TCDD in both cell lines, although

the magnitude of induction is greater in HepG2 cells (mean \pm SD, 2.33 ± 0.25 and 8.90 ± 2.75 respectively). When the DRE sites were mutated the TCDD-responsiveness dropped considerably. Interestingly, we found that the decrease in inducibility of the reporter construct harboring the mutated sites was not as pronounced in the RWPE-1 cells relative to HepG2 cells (30% vs. 72% decrease, respectively). The low level of TCDD-responsiveness observed in the pGL3-38k-mut reporter construct is probably due to a low affinity DRE site (5'-GTGCGTG-3') centered at -38,116 relative to *CYP1A1*'s transcriptional start site. These findings, together with the results of our ChIP and *in vivo* footprinting experiments (Figs 2 and 3), indicate that *CYP1A2*'s 3' region can function as a TCDD-responsive AhR-dependent enhancer.

Analysis of other human cell lines. We extended our analysis of the native *CYP1A* locus by studying three additional human cell lines. We analyzed LS180 cells (colon adenocarcinoma) and HepG2 cells (hepatocellular carcinoma) which are inducible for *CYP1A2* (Li et al., 1998) as well as ND-1 cells (prostate adenocarcinoma) which represent a cancerous counterpart to the non-cancerous RWPE-1 prostate cells. Analysis of RNA induction by both conventional PCR and real-time PCR reveals that *CYP1A2* is strongly induced in RWPE-1, LS180 and HepG2 cells whereas induction is barely detectable in ND-1 cells (Fig 5a, Table 1). All of the cell lines induce *CYP1A1* RNA, however in ND-1 cells the fold-induction and level of induced *CYP1A1* RNA is significantly lower than that found in the other cell lines (Fig 5a, Table 1).

ChIP analysis of the *CYP1A* locus reveals that AHR binds to *CYP1A2*'s 3' enhancer in TCDD-treated RWPE-1 and LS180 cells; thus the activity of *CYP1A2*'s 3' enhancer is not restricted to a single cell line. In contrast, in HepG2 and ND-1 cells AhR does not bind to *CYP1A2*'s 3' region (Fig. 5b). These findings imply that AhR binding to *CYP1A2*'s 3' region is associated with *CYP1A2* induction, but is not required. In all cell lines AhR binds to *CYP1A1*'s enhancer following TCDD treatment. We do not detect AhR binding at other *CYP1A* DRE sites.

We also analyzed histone H4 acetylation on the *CYP1A* locus by ChIP. Previously, we and others demonstrated that TCDD increases histone H4 acetylation on the *CYP1A1* regulatory region (Ke et al., 2001; Hestermann and Brown, 2003; Okino et al., 2006). Our results show that in the three cell lines that strongly induce *CYP1A1* and *CYP1A2* (RWPE-1, LS180 and HepG2) TCDD treatment increases histone H4 acetylation along the entire 75 kb *CYP1A* locus. In contrast, in ND-1 cells where *CYP1A1* but not *CYP1A2* is inducible, only the chromatin in the immediate vicinity of *CYP1A1* exhibits increased histone H4 acetylation. These results reveal a strong association between induced histone acetylation and induced gene activity.

We suspected that AhR's inability to interact with *CYP1A2*'s 3' region in HepG2 and ND-1 cells might be associated with DNA methylation. Previously we demonstrated that DNA methylation on *CYP1A1*'s enhancer prevents AhR-binding and inhibits *CYP1A1* induction in human prostate cancer (Okino et al., 2006); others have shown that *CYP1A2*'s promoter is methylated in mouse tissues (Jin et al., 2004). Our analysis of DNA methylation (Fig 5c and data not shown) reveals that all CpG within the region analyzed (between -37,900 and -38,125 relative to *CYP1A1*'s transcription start site) are completely methylated in HepG2 and ND-1 cells. In contrast, no methylation is detected in RWPE-1 and LS180 cells. Importantly, in HepG2 and ND-1 cells the CpG site within DRE-1 is completely methylated; such methylation was previously shown to inhibit AhR interaction *in vitro* and *in vivo* (Shen and Whitlock, 1989). We infer that DNA methylation inactivates the TCDD-responsive enhancer 3' of *CYP1A2* in HepG2 and ND-1 cells.

Discussion

The members of the *CYP1* gene family, *CYP1A1*, *CYP1A2* and *CYP1B1*, are transcriptionally induced by the AhR. Although the TCDD-responsive, AhR-dependent enhancers for *CYP1A1* and *CYP1B1* are well characterized, details regarding a similar *CYP1A2* enhancer remained elusive (Hankinson, 1995; Whitlock et al., 1997; Nebert and Dalton, 2006). Here we demonstrate that DRE sites 3' of the native *CYP1A2* gene bind AhR in TCDD-treated human prostate and colon cells and function as a TCDD-responsive enhancer in a reporter gene assay. We infer that this region participates in TCDD-induction of *CYP1A2* in humans and is thus a *bona fide* *CYP1A2* enhancer.

Unlike the dioxin-responsive enhancers for *CYP1A1* and *CYP1B1* which are positioned about 1 kb upstream of their respective genes, the *CYP1A2* enhancer is downstream of *CYP1A2* and further away, about 15 kb away from the *CYP1A2*'s transcriptional start site. There is precedence for an enhancer being located downstream of its target gene; there is also precedence for an enhancer being located distant, up to 100 kb away, from the promoter that it controls (Blackwood and Kadonaga, 1998; Carroll et al., 2005; Maston et al., 2006). Therefore, although the placement and distance of the *CYP1A2*'s enhancer is unique among characterized AhR-regulated genes, it is not unusual in the context of general enhancer action.

It is significant that HepG2 cells induce *CYP1A2* in the absence of AhR binding to its 3' enhancer (Fig 5). This implies that binding to this enhancer is not required for *CYP1A2* induction. Consistent with this, a cross-species DNA sequence homology comparison shows that the DRE sites within this region are not well-conserved in other species (Fig 6). Again, this implies that the *CYP1A2* enhancer identified in this study is not required for TCDD-induction of *CYP1A2*. Therefore, another enhancer likely controls *CYP1A2*. Interestingly, we find that two closely spaced DRE sites located just 1 kb away from the identified *CYP1A2* enhancer exhibit cross-species conservation at a level similar to that found in the *CYP1A1* and *CYP1B1* enhancers (Fig 6). This suggests that this region may participate in TCDD-regulation. However, our ChIP data clearly shows that these DREs, located at -37 kb relative to the *CYP1A1* transcriptional start site, do not bind AhR in any cell line tested (Fig 5b). Not surprisingly,

analysis of DNA methylation shows that both DRE sites are completely methylated in RWPE-1, LS180, HepG2 and ND-1 cells (data not shown). Thus, DNA methylation likely suppresses the TCDD-responsiveness of this region. We suspect that the growth of cells as a monolayer culture inactivates this region. Indeed, the expression of *CYP1A2* in primary hepatocytes is known to dramatically decrease over time while the extent of *CYP1A2* promoter methylation increases (Nemoto and Sakurai, 1993; Jin et al., 2004). Future studies that determine the significance of this putative control region may provide novel insights into *CYP1A2* regulation

We have identified a TCDD-responsive *CYP1A2* enhancer that can be regulated by DNA methylation and is primarily human-specific. We believe that expression of *CYP1A2* in humans involves coordination between this enhancer, *CYP1A1*'s enhancer, *CYP1A2*'s promoter and the putative *CYP1A2* regulatory region described above. Obviously, control of *CYP1A2* is quite complex and involves multiple regulatory regions and a layer of epigenetic control. Also, based upon the species specificity of this enhancer, TCDD-regulation of *CYP1A2* is likely to differ between humans and most other animal species.

PAHs are toxic and carcinogenic compounds that are ubiquitous in the environment and prevalent in cigarette smoke, automobile exhaust and in charcoal-cooked meats. PAH exposure activates AhR and induces the expression of the *CYP1* genes. The *CYP1* gene products initiate PAH metabolism through oxidation (Poland and Knutson, 1982; Whitlock et al., 1997). Following oxidation, the PAHs are further modified by conjugation with glutathione, ultimately leading to their detoxification and elimination from the body. Studies in knockout mice reveal that induction of *CYP1A1* and *CYP1A2* is advantageous because animals that lack them are acutely sensitive to chemical toxicity. In contrast, *CYP1B1* induction has an adverse effect because *Cyp1b1*^{-/-} animals are protected against PAH toxicity (Nebert et al., 2004; Nebert and Dalton, 2006). Our previous work revealed that some prostate tumors are likely unable to induce *CYP1A1* because its enhancer is silenced by DNA hypermethylation (Okino et al., 2006). In contrast, *CYP1B1* is overexpressed in prostate tumors due to gene hypomethylation (Tokizane et al., 2005). Here we show that induction of *CYP1A2*, like *CYP1A1*, may be silenced by enhancer hypermethylation in human prostate cancer. Thus, in prostate tumors two genes that protect against

chemical toxicity are suppressed and a gene that mediates PAH toxicity is overexpressed. The combined effect likely results in increased sensitivity to PAH toxicity. To compound this, two glutathione-S-transferases that detoxify PAHs are not expressed in most prostate cancers because their genes, *GSTP1* and *GSTM1*, are inactivated by DNA hypermethylation (Harden et al., 2003; Nakayama et al., 2004; Lodygin et al., 2005). Thus, some prostate tumors are likely to exhibit acute sensitive to adverse PAH effects. Indeed, several large epidemiological studies demonstrate that smokers, a group that has high PAH exposure, have higher prostate cancer-associated mortality (Rodriguez et al., 1997; Giovannucci et al., 1999; Doll et al., 2005). Future epidemiological studies that assess DNA methylation on genes involved in xenobiotic metabolism may provide insights into this intriguing observation.

Acknowledgements

We thank Robert Place and Roger Erickson for critical review of this manuscript.

References

- Blackwood EM and Kadonaga JT (1998) Going the distance: a current view of enhancer action. *Science* **281**:60-63.
- Carroll JS, Liu XS, Brodsky AS, Li W, Meyer CA, Szary AJ, Eeckhoutte J, Shao W, Hestermann EV, Geistlinger TR, Fox EA, Silver PA and Brown M (2005) Chromosome-wide mapping of estrogen receptor binding reveals long-range regulation requiring the forkhead protein FoxA1. *Cell* **122**:33-43.
- Corchero J, Pimprale S, Kimura S and Gonzalez FJ (2001) Organization of the CYP1A cluster on human chromosome 15: implications for gene regulation. *Pharmacogenetics* **11**:1-6.
- Doll R, Peto R, Boreham J and Sutherland I (2005) Mortality from cancer in relation to smoking: 50 years observations on British doctors. *Br J Cancer* **92**:426-429.
- Giovannucci E, Rimm EB, Ascherio A, Colditz GA, Spiegelman D, Stampfer MJ and Willett WC (1999) Smoking and risk of total and fatal prostate cancer in United States health professionals. *Cancer Epidemiol Biomarkers Prev* **8**:277-282.
- Hankinson O (1995) The aryl hydrocarbon receptor complex. *Annu Rev Pharmacol Toxicol* **35**:307-340.
- Harden SV, Sanderson H, Goodman SN, Partin AA, Walsh PC, Epstein JI and Sidransky D (2003) Quantitative GSTP1 methylation and the detection of prostate adenocarcinoma in sextant biopsies. *J Natl Cancer Inst* **95**:1634-1637.
- Hestermann EV and Brown M (2003) Agonist and chemopreventative ligands induce differential transcriptional cofactor recruitment by aryl hydrocarbon receptor. *Mol Cell Biol* **23**:7920-7925.

- Jiang Z, Dalton TP, Jin L, Wang B, Tsuneoka Y, Shertzer HG, Deka R and Nebert DW (2005)
Toward the evaluation of function in genetic variability: characterizing human SNP
frequencies and establishing BAC-transgenic mice carrying the human
CYP1A1_CYP1A2 locus. *Hum Mutat* **25**:196-206.
- Jin B, Park DW, Nam KW, Oh GT, Lee YS and Ryu DY (2004) CpG methylation of the mouse
CYP1A2 promoter. *Toxicol Lett* **152**:11-18.
- Ke S, Rabson AB, Germino JF, Gallo MA and Tian Y (2001) Mechanism of suppression of
cytochrome P-450 1A1 expression by tumor necrosis factor-alpha and
lipopolysaccharide. *J Biol Chem* **276**:39638-39644.
- Kent WJ, Sugnet CW, Furey TS, Roskin KM, Pringle TH, Zahler AM and Haussler D (2002)
The human genome browser at UCSC. *Genome Res* **12**:996-1006.
- Kress S, Reichert J and Schwarz M (1998) Functional analysis of the human cytochrome
P4501A1 (CYP1A1) gene enhancer. *Eur J Biochem* **258**:803-812.
- Li W, Harper PA, Tang BK and Okey AB (1998) Regulation of cytochrome P450 enzymes by
aryl hydrocarbon receptor in human cells: CYP1A2 expression in the LS180 colon
carcinoma cell line after treatment with 2,3,7,8-tetrachlorodibenzo-p-dioxin or 3-
methylcholanthrene. *Biochem Pharmacol* **56**:599-612.
- Lodygin D, Epanchintsev A, Menssen A, Diebold J and Hermeking H (2005) Functional
epigenomics identifies genes frequently silenced in prostate cancer. *Cancer Res* **65**:4218-
4227.
- Maston GA, Evans SK and Green MR (2006) Transcriptional Regulatory Elements in the Human
Genome. *Annu Rev Genomics Hum Genet* **7**:29-59.

- Nakayama M, Gonzalgo ML, Yegnasubramanian S, Lin X, De Marzo AM and Nelson WG (2004) GSTP1 CpG island hypermethylation as a molecular biomarker for prostate cancer. *J Cell Biochem* **91**:540-552.
- Narayan P and Dahiya R (1992) Establishment and characterization of a human primary prostatic adenocarcinoma cell line (ND-1). *J Urol* **148**:1600-1604.
- Nebert DW and Dalton TP (2006) The role of cytochrome P450 enzymes in endogenous signalling pathways and environmental carcinogenesis. *Nat Rev Cancer* **6**:947-960.
- Nebert DW, Dalton TP, Okey AB and Gonzalez FJ (2004) Role of aryl hydrocarbon receptor-mediated induction of the CYP1 enzymes in environmental toxicity and cancer. *J Biol Chem* **279**:23847-23850.
- Nemoto N and Sakurai J (1993) Activation of Cyp1a1 and Cyp1a2 genes in adult mouse hepatocytes in primary culture. *Jpn J Cancer Res* **84**:272-278.
- Okino ST, Pookot D, Li LC, Zhao H, Urakami S, Shiina H, Igawa M and Dahiya R (2006) Epigenetic inactivation of the dioxin-responsive cytochrome P4501A1 gene in human prostate cancer. *Cancer Res* **66**:7420-7428.
- Okino ST and Whitlock JP, Jr. (1995) Dioxin induces localized, graded changes in chromatin structure: implications for Cyp1A1 gene transcription. *Mol Cell Biol* **15**:3714-3721.
- Poland A and Knutson JC (1982) 2,3,7,8-tetrachlorodibenzo-p-dioxin and related halogenated aromatic hydrocarbons: examination of the mechanism of toxicity. *Annu Rev Pharmacol Toxicol* **22**:517-554.
- Postlind H, Vu TP, Tukey RH and Quattrochi LC (1993) Response of human CYP1-luciferase plasmids to 2,3,7,8-tetrachlorodibenzo-p-dioxin and polycyclic aromatic hydrocarbons. *Toxicol Appl Pharmacol* **118**:255-262.

- Quattrochi LC and Tukey RH (1989) The human cytochrome Cyp1A2 gene contains regulatory elements responsive to 3-methylcholanthrene. *Mol Pharmacol* **36**:66-71.
- Quattrochi LC, Vu T and Tukey RH (1994) The human CYP1A2 gene and induction by 3-methylcholanthrene. A region of DNA that supports AH-receptor binding and promoter-specific induction. *J Biol Chem* **269**:6949-6954.
- Rodriguez C, Tatham LM, Thun MJ, Calle EE and Heath CW, Jr. (1997) Smoking and fatal prostate cancer in a large cohort of adult men. *Am J Epidemiol* **145**:466-475.
- Schmidt JV and Bradfield CA (1996) Ah receptor signaling pathways. *Annu Rev Cell Dev Biol* **12**:55-89.
- Shen ES and Whitlock JP, Jr. (1989) The potential role of DNA methylation in the response to 2,3,7,8-tetrachlorodibenzo-p-dioxin. *J Biol Chem* **264**:17754-17758.
- Shimada T and Fujii-Kuriyama Y (2004) Metabolic activation of polycyclic aromatic hydrocarbons to carcinogens by cytochromes P450 1A1 and 1B1. *Cancer Sci* **95**:1-6.
- Swanson HI, Chan WK and Bradfield CA (1995) DNA binding specificities and pairing rules of the Ah receptor, ARNT, and SIM proteins. *J Biol Chem* **270**:26292-26302.
- Tokizane T, Shiina H, Igawa M, Enokida H, Urakami S, Kawakami T, Ogishima T, Okino ST, Li LC, Tanaka Y, Nonomura N, Okuyama A and Dahiya R (2005) Cytochrome P450 1B1 is overexpressed and regulated by hypomethylation in prostate cancer. *Clin Cancer Res* **11**:5793-5801.
- Tsuchiya Y, Nakajima M and Yokoi T (2003) Critical enhancer region to which AhR/ARNT and Sp1 bind in the human CYP1B1 gene. *J Biochem (Tokyo)* **133**:583-592.

- Ueda R, Iketaki H, Nagata K, Kimura S, Gonzalez FJ, Kusano K, Yoshimura T and Yamazoe Y (2006) A common regulatory region functions bidirectionally in transcriptional activation of the human CYP1A1 and CYP1A2 genes. *Mol Pharmacol* **69**:1924-1930.
- Whitlock JP, Jr. (1999) Induction of cytochrome P4501A1. *Annu Rev Pharmacol Toxicol* **39**:103-125.
- Whitlock JP, Jr., Chichester CH, Bedgood RM, Okino ST, Ko HP, Ma Q, Dong L, Li H and Clarke-Katzenberg R (1997) Induction of drug-metabolizing enzymes by dioxin. *Drug Metab Rev* **29**:1107-1127.
- Wu L and Whitlock JP, Jr. (1993) Mechanism of dioxin action: receptor-enhancer interactions in intact cells. *Nucleic Acids Res* **21**:119-125.
- Yueh MF, Kawahara M and Raucy J (2005) Cell-based high-throughput bioassays to assess induction and inhibition of CYP1A enzymes. *Toxicol In Vitro* **19**:275-287.
- Zhang L, Savas U, Alexander DL and Jefcoate CR (1998) Characterization of the mouse Cyp1B1 gene. Identification of an enhancer region that directs aryl hydrocarbon receptor-mediated constitutive and induced expression. *J Biol Chem* **273**:5174-5183.

Footnotes

Grant support: NIH grants RO1CA101844, RO1CA111470, RO1CA108612, RO1AG21418, and T32DK07790, VA Merit Review and REAP grants. Address reprint requests to: Rajvir Dahiya, Department of Urology, San Francisco Veterans Affairs Medical Center and UCSF, 4150 Clement Street, Building 203 room 2B-24 (112F), San Francisco, CA 94121. E-mail: Rdahiya@urology.ucsf.edu

Legends for Figures

Figure 1. TCDD induction of CYP1 mRNAs in RWPE-1 cells. RNA isolated from untreated or TCDD treated (10 nM, 18 hours) RWPE-1 cells was analyzed by RT-PCR to assess the level of CYP1A2, CYP1A1, CYP1B1, AhR, Arnt and glyceraldehyde-3-phosphate dehydrogenase (GAPDH) RNA. CYP1A2 RNA was amplified for 35 PCR cycles; CYP1A1, CYP1B1, AhR and Arnt RNA were amplified for 30 PCR cycles; GAPDH RNA was amplified for 28 PCR cycles.

Figure 2. AhR interaction with the *CYP1A* locus. A, A schematic depiction of a 75 kb region that encompasses the human *CYP1A* locus. The coding regions of *CYP1A1* and *CYP1A2* are in grey and the direction of transcription is indicated. High affinity AhR binding sites are indicated (black lines) along with the approximate distance, in kilobases (kb), from the *CYP1A1* transcriptional start site. For closely spaced AhR binding sites, the number of sites is indicated in parenthesis. The location of the *CYP1A1* enhancer is also indicated (*). B, AhR binding on the *CYP1A* locus, the *CYP1B1* gene and the *GAPDH* gene was assessed in untreated and TCDD-treated (10 nM, 1 hour) RWPE-1 cells by ChIP. Enhancer (En) and promoter (Pro) regions are indicated. C, AhR binding on *CYP1A2*'s 3' enhancer, the *CYP1A1* enhancer, the *CYP1B1* enhancer and the *GAPDH* promoter was assessed in RWPE-1 cells treated with TCDD (10 nM) for the indicated length of time by ChIP.

Figure 3. TCDD-inducible occupancy of AhR binding sites on *CYP1A2*'s 3' enhancer. A, Sequence of the human *CYP1A2* 3' enhancer region. High affinity DRE sites are in bold. The DNA regions used to design primers used for ChIP and LMPCR primer 3 are indicated (boxed). The DNA region cloned into pGL3-38k-wt is indicated (italics) and the base changes used in the construction of pGL3-38k-mut are shown (below sequence). Filled arrows indicate sites hypersensitive to DMS modification following TCDD treatment. Open arrows indicate sites hyposensitive to DMS modification following TCDD treatment. The distance, in base pairs, from the *CYP1A1* transcriptional start site is also indicated. B, Untreated or TCDD-induced (10 nM, 1 hour) RWPE-1 cells were treated with 0.1 % DMS for 90

seconds. Genomic DNA was isolated and the pattern and extent of DMS modification was assessed by LMPCR. N; naked genomic DNA treated with DMS *in-vitro*. -; genomic DNA isolated from untreated cells. +; genomic DNA isolated from TCDD-induced cells. Filled arrows indicate sites hypersensitive to DMS modification following TCDD treatment. Open arrows indicate sites hyposensitive to DMS modification following TCDD treatment. DRE sites and the distance, in base pairs from the *CYP1A1* transcriptional start site are also indicated.

Figure 4. Reporter gene analysis of *CYP1A2*'s 3' enhancer. Expression of pGL3-38k-wt (38N) and pGL3-38k-mut (38X) in RWPE-1 and HepG2 cells. *CYP1A2* 3'-flanking sequences containing AhR binding sites and mutations of those sites were cloned into the pGL3-promoter plasmid and transfected into cell lines as described under *Materials and Methods*. pDRE12 (DRE), containing three copies of the consensus DRE subcloned into the pGL3-promoter vector, was used as a control. DMSO and TCDD treatments were performed 24 h after transfection; the cells were harvested and assayed for luciferase activity 24 h after chemical treatment. The amount of *Firefly* luciferase activity was normalized against *Renilla* luciferase activities of the pRL-SV40 vector obtained from the same culture. Data are presented as the ratio of luciferase activity of treated cells to DMSO control cells and represent the mean \pm SD from three experiments performed in triplicate. *, denotes statistical significance ($p < 0.05$) of each reporter construct *versus* 38N.

Figure 5. Analysis of a several human cell lines. A, RNA isolated from untreated or TCDD treated (10 nM, 18 hours) cells was analyzed by RT-PCR to assess the level of *CYP1A2*, *CYP1A1* and *GAPDH* RNA. *CYP1A2* RNA was amplified for 35 PCR cycles, *CYP1A1* RNA was amplified for 30 PCR cycles, *GAPDH* RNA was amplified for 28 PCR cycles. B, AhR binding and histone H4 acetylation on the *CYP1A* locus and *GAPDH* promoter was assessed in untreated and TCDD-treated (10 nM, 1 hour) cells by ChIP. The no antibody and input controls for these reactions are presented in supplementary data figure 1. C, DNA methylation on *CYP1A2*'s 3' enhancer was assessed by bisulfite DNA sequencing. The

black lines indicate 5-methylcytosine; the red lines indicate adenine; the green lines indicate thymine and unmethylated cytosine; the blue lines indicate guanine; red asterisks indicates sites containing significant levels of 5-methylcytosine. The location of DRE 1 and the distance from the *CYP1A1* transcriptional start site is indicated. Note that the sequencing reaction reads the complimentary strand of the sequence presented in figure 3a.

Figure 6. Cross-species comparison of DNA homology. *A*, The cross-species homology of specific DNA regions was compared using the vertebrate multiz alignment and conservation track on the UCSC Genome browser (<http://genome.ucsc.edu/>) (Kent et al., 2002). DRE sites are in bold. Dots represent bases identical to the corresponding human base. Single line: no bases in the aligned region. Double line: aligning species has one or more unalignable bases in the gap region. Species name in bold type indicates that both AhR binding sites are conserved. *B*, Cross-species conservation of AhR binding sites. Yes indicates that both AhR binding sites are conserved in a particular species. No indicates that the core AhR-binding motif of at least one site is not conserved in a particular species.

Tables

Table 1. Quantitation of CYP1A RNA levels. CYP1A1, CYP1A2 and GAPDH RNA levels were estimated by real-time PCR. The fold TCDD induction was calculated as the ratio of induced CYP1A RNA to basal CYP1A RNA. The induced RNA level was calculated as (induced CYP1A RNA level/corresponding GAPDH RNA level) x 100. The liver and prostate RNA data were from analysis of a single sample. The other results represent an average of two independent samples. No information regarding the TCDD/xenobiotic exposure of the liver and prostate RNA donors is known, thus only the level of CYP1A RNA relative to GAPDH is reported.

	Fold TCDD induction		Induced RNA level (% of GAPDH RNA level)	
	CYP1A1	CYP1A2	CYP1A1	CYP1A2
RWPE-1	310	45	60%	0.020%
LS180	6,700	3,300	65%	0.700%
HepG2	440	210	73%	0.132%
ND-1	8	2	0.1%	0.002%
Liver	-	-	4.6%	49%
Prostate	-	-	2%	0.053%

Figure 1

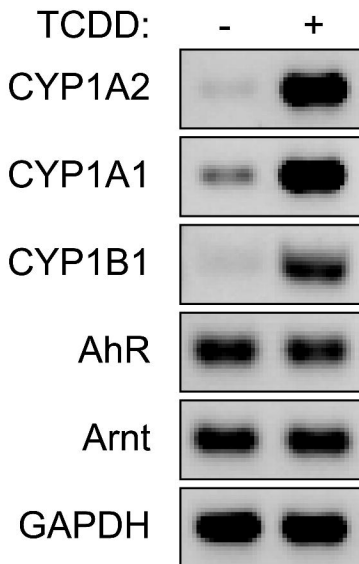
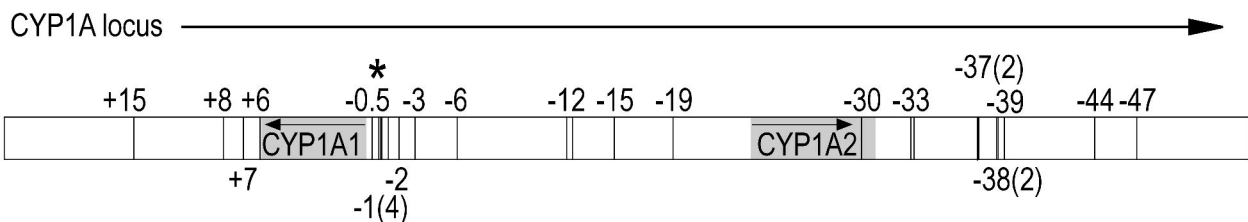
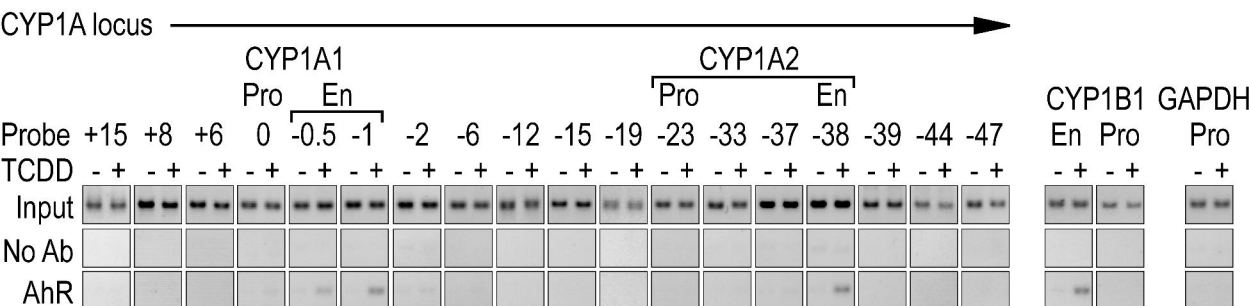


Figure 2

A



B



C

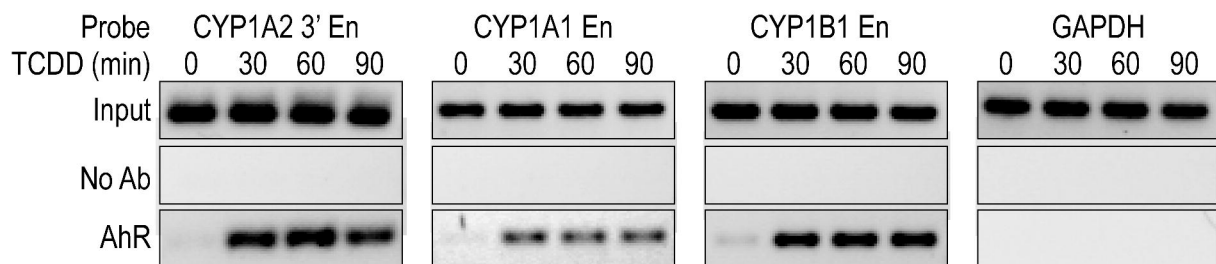
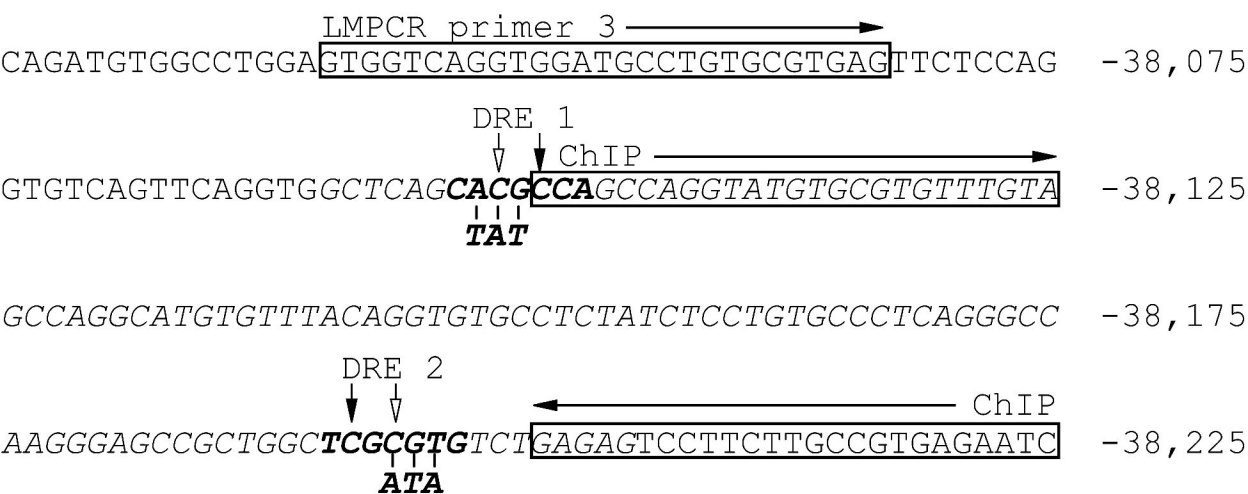


Figure 3

A



B

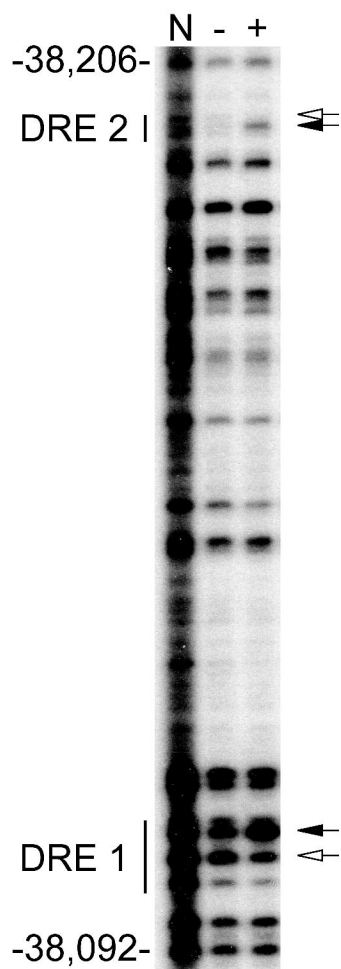


Figure 4

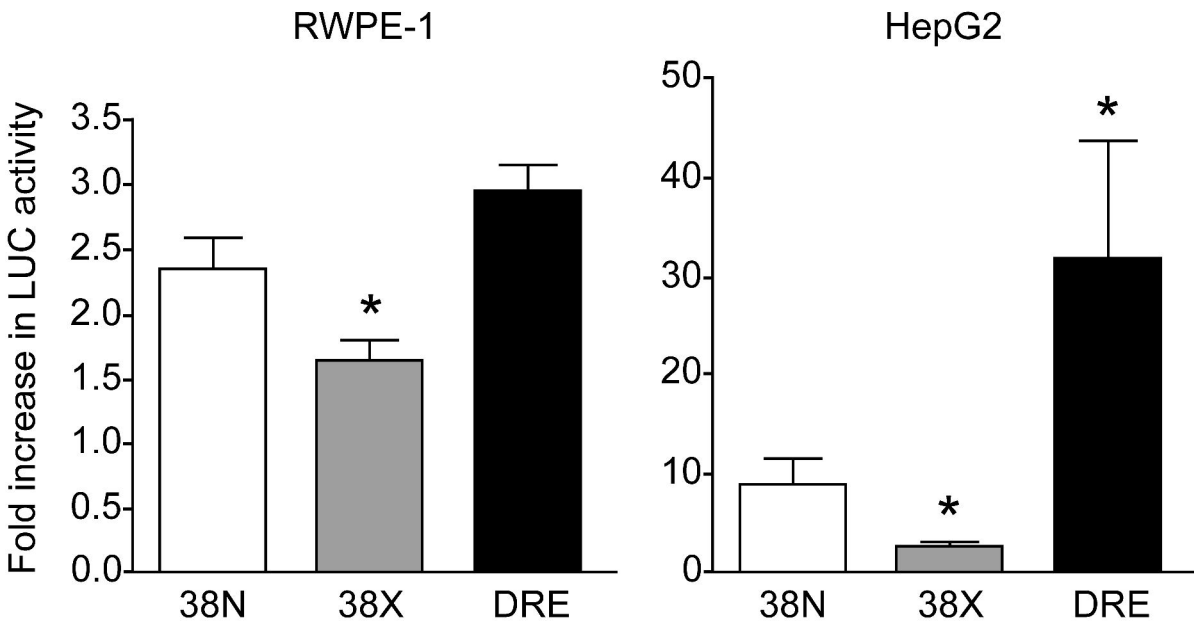
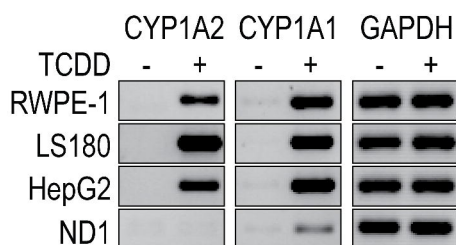
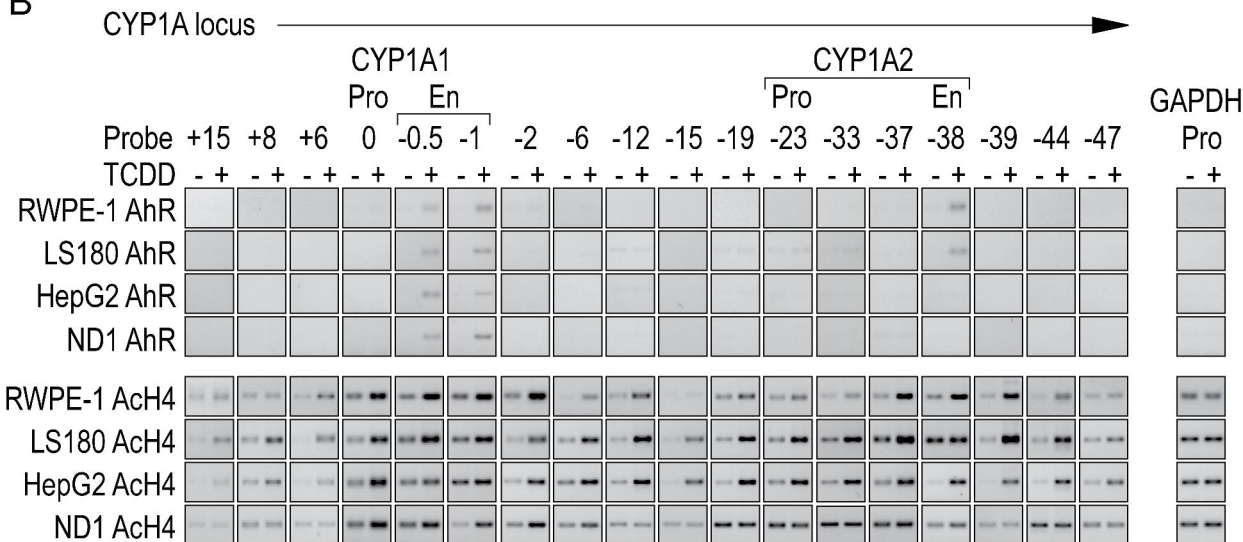


Figure 5

A



B



C

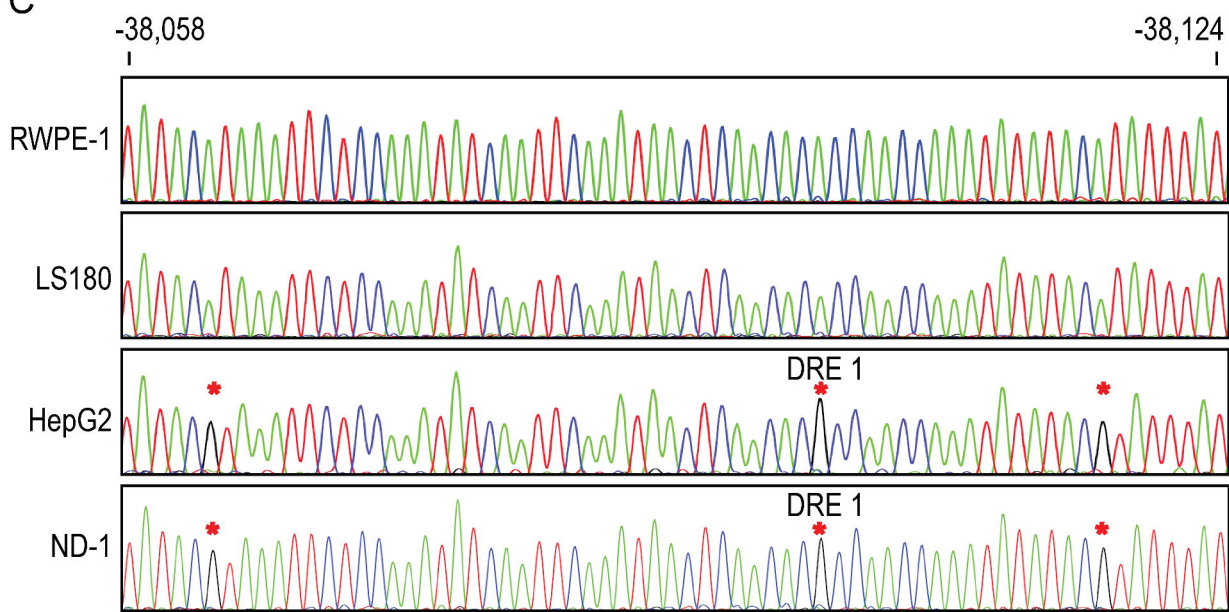
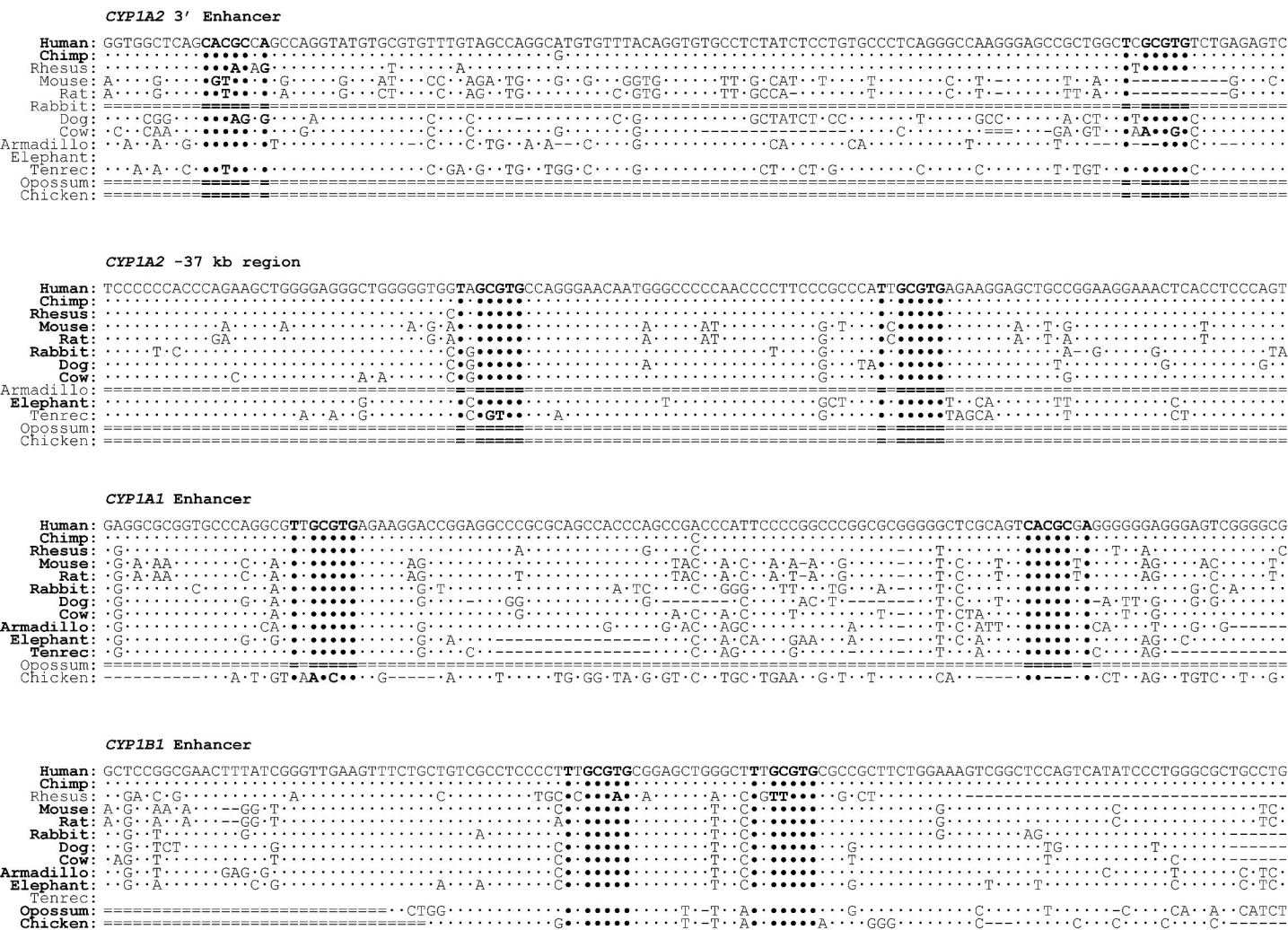


Figure 6

A



B

